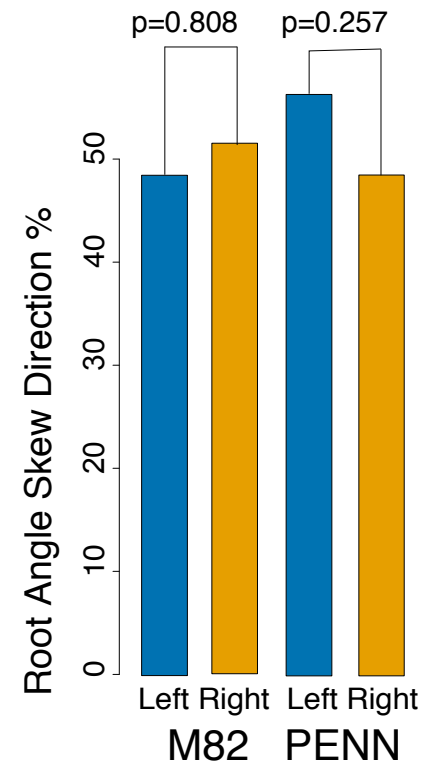
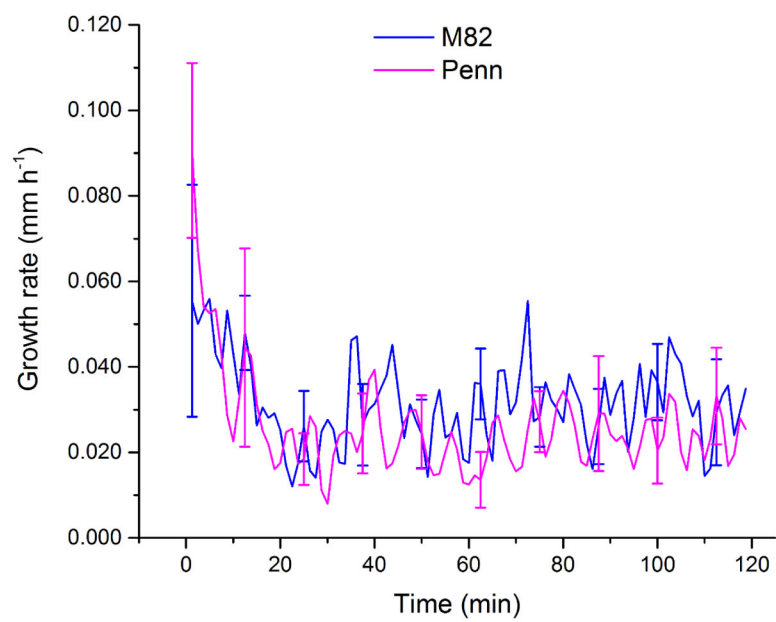
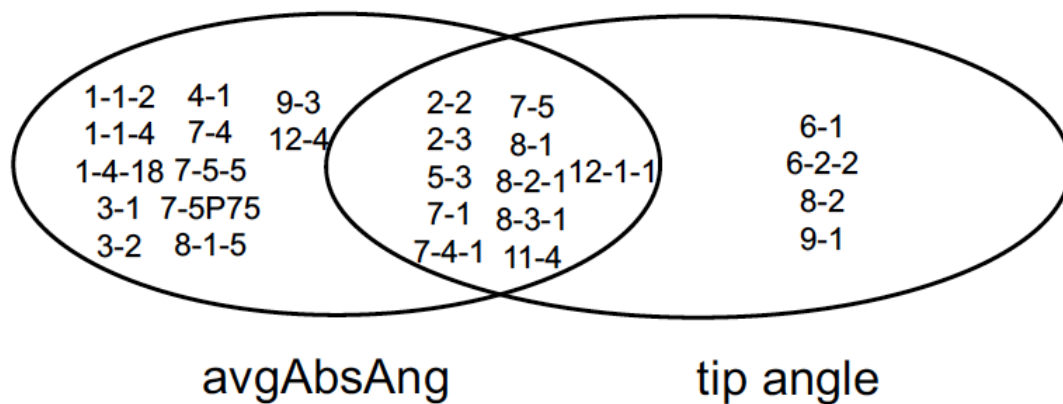


**Figure S1.** Changes in Root angle in M82 and Penn do not represent skewing. Percentage of roots (y-axis) showing skew to the left or to the right in M82 (n=68) and PENN (n=78). No preference to skew to the left or the right is observed using a chi-square test and thus the null hypothesis is accepted.

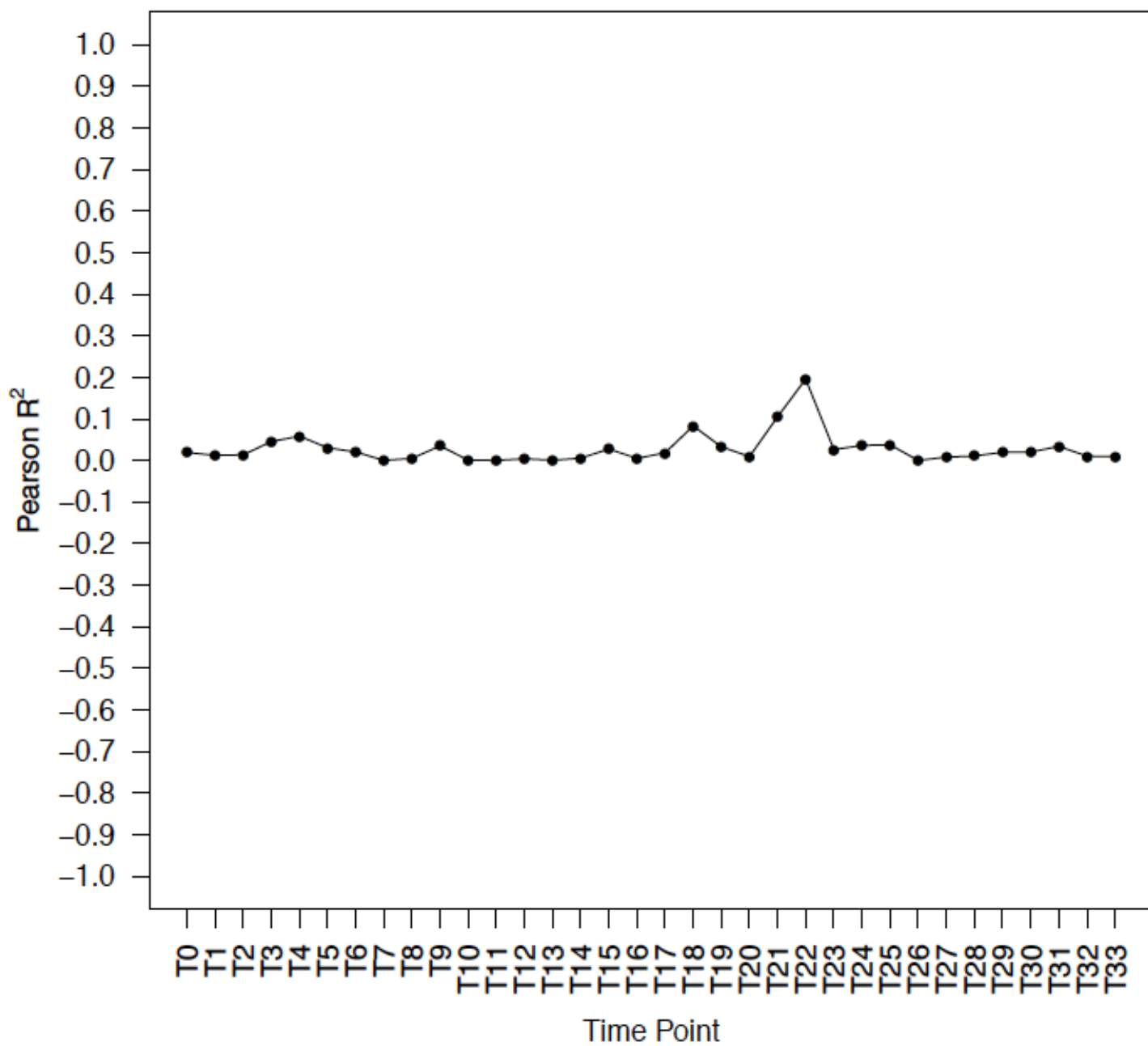


**Figure S2: Mean root growth rate per time point in the two hours following rotation of M82 (n=89) and PENN (n=18).**

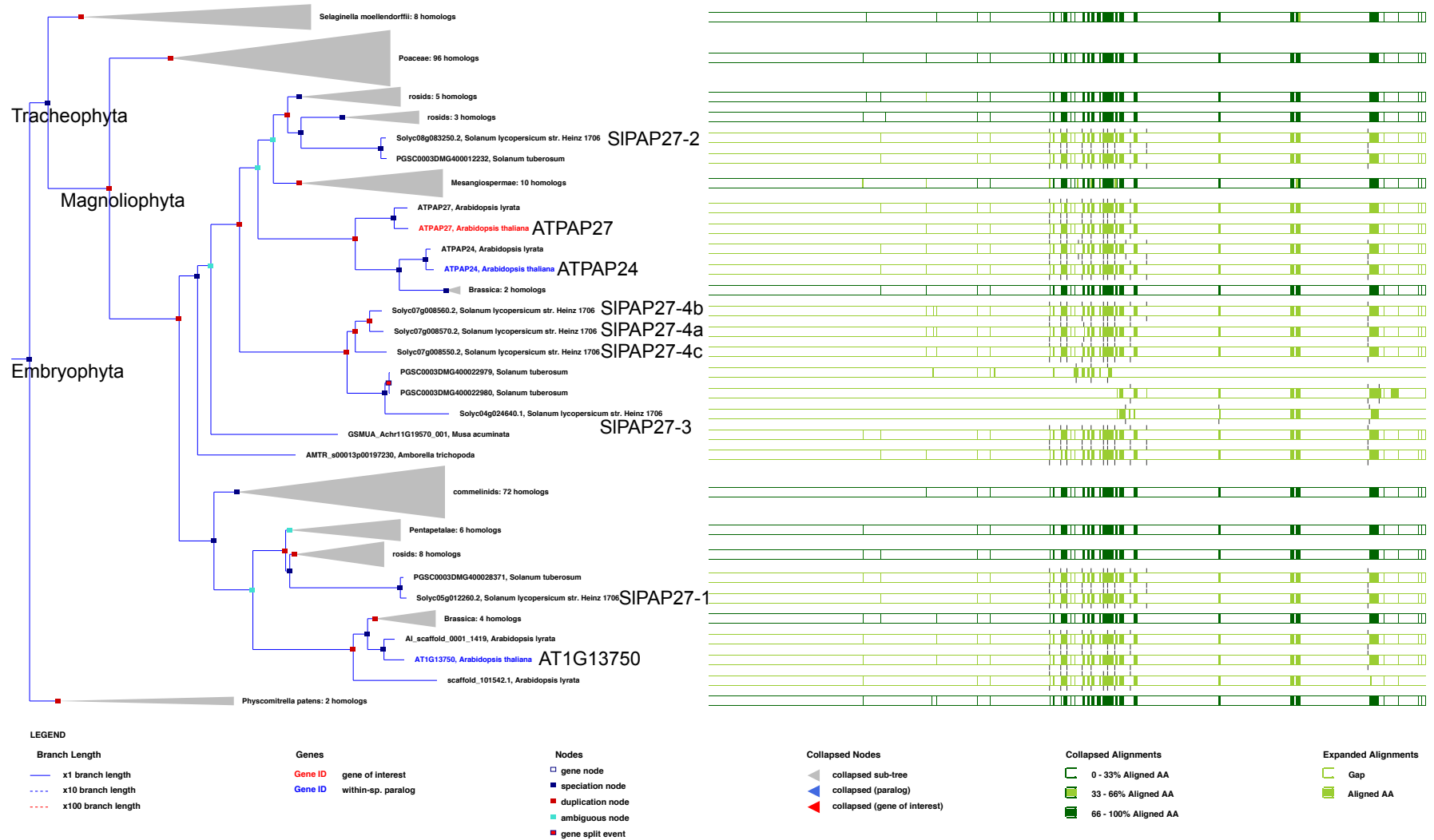




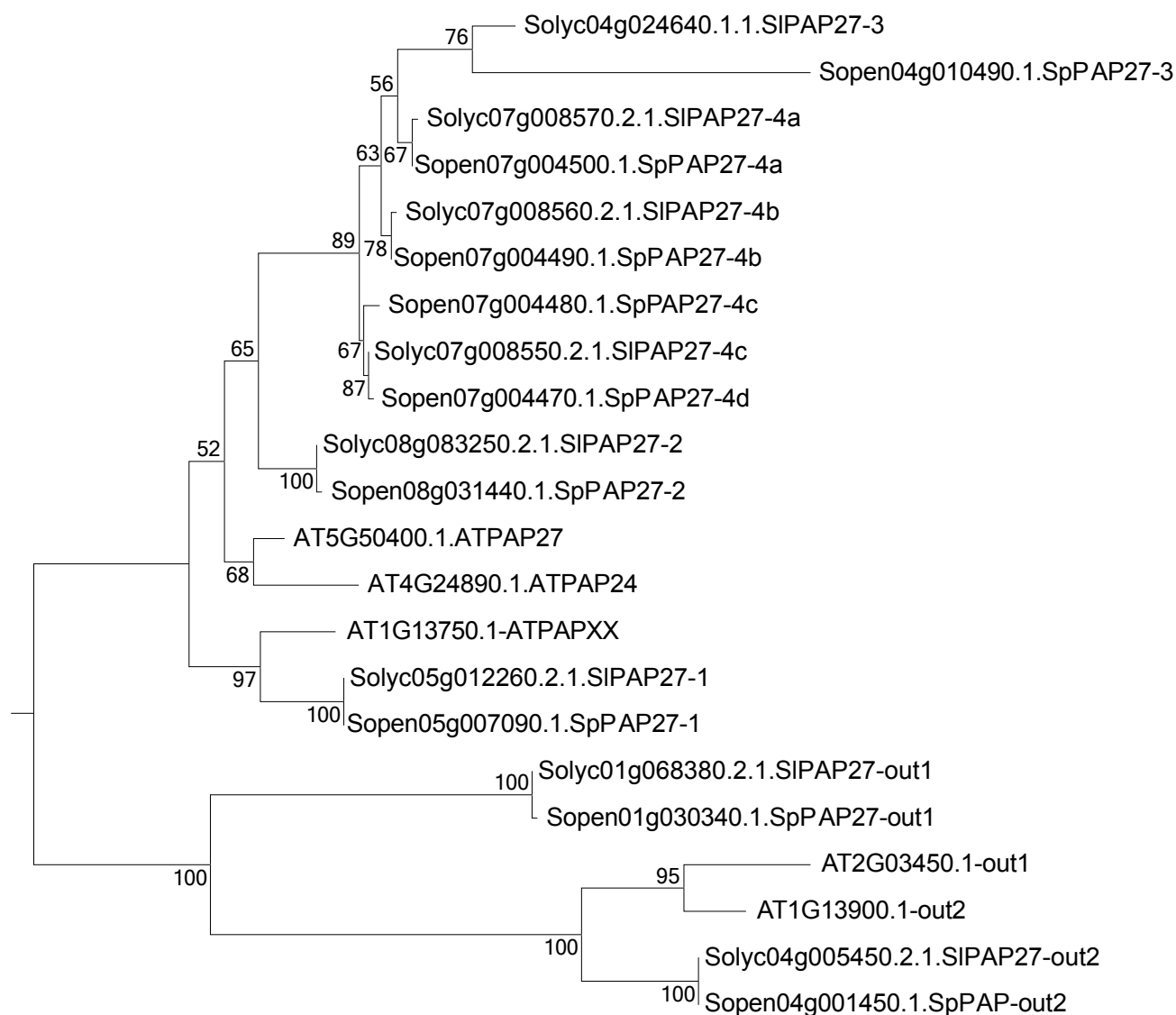
**Figure S3.** Overlap between average absolute angle QTL and root tip angle QTL. Venn diagram showing overlap between QTL identified for average absolute angle in this study compared to Ron et al. 2013.



**Figure S4.** Pearson correlation of avgAbsAng with swing rate at each of the 34 time points.

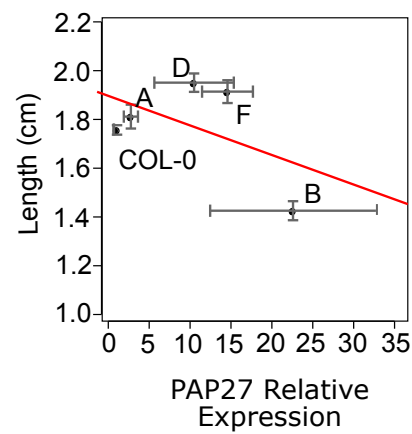


**Figure S5: Precomputed phylogenetic tree of *AT5G50400* (*PAP27*) and homologs in different species.** Homology to the protein sequence of *AT5G50400* [111, 112] is used. The taxon designation of the three highest nodes is shown. Subnodes that do not contain any genes from *A. thaliana* or *S. lycopersicum* are collapsed. *PAP27* and its paralogs in *A. thaliana* and homologs in *S. lycopersicum* are called out in larger type. Alignments are shown to the right.

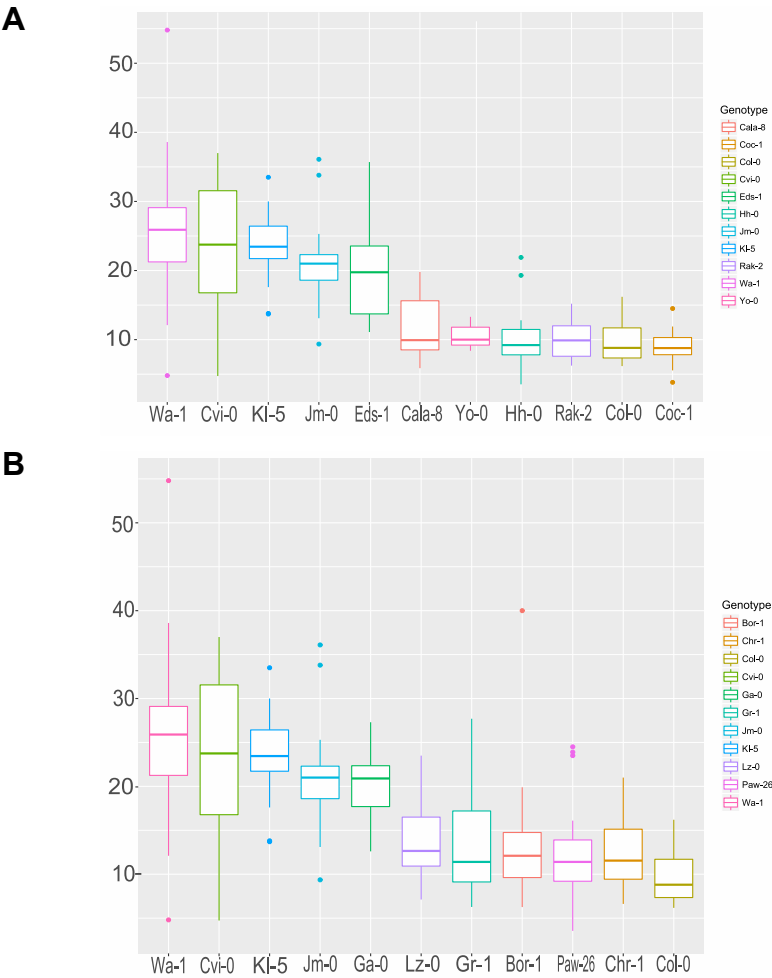


**Figure S5: Maximum likelihood phylogenetic tree of *AT5G50400* (PAP27) and homologs in *A. thaliana*, *S. lycopersicum*, and *S. pennellii*.** Tree is computed with 200 bootstraps using MEGA (Tamura et al. 2011) from protein sequences. Suffixes "-out1" and "-out2" mark genes used as outgroups. Homologs were identified using the gene tree from Figure S5 and with BLAST+ (Camacho et al. 2009). Multiple alignment used Muscle (Edgar 2004).

**Figure S7. Root Length of *AtPAP27* overexpression lines does not linearly correlate with expression of *AtPAP27*.** Error bars represent standard error of the mean,  $n_{\text{avgAbsAng}}(\text{Col-0})=275$ ,  $n_{\text{avgAbsAng}}(35\text{S:AtPAP27/lineA})=11$ ,  $n_{\text{avgAbsAng}}(35\text{S:AtPAP27/lineB})=20$ ,  $n_{\text{avgAbsAng}}(35\text{S:AtPAP27/lineD})=83$ ,  $n_{\text{avgAbsAng}}(35\text{S:AtPAP27/lineF})=100$ ;  $n_{\text{EXPRESSION}}(\text{Col-0})=$ ,  $n_{\text{EXPRESSION}}(35\text{S:AtPAP27/lineA})=11$ ,  $n_{\text{EXPRESSION}}(35\text{S:AtPAP27/lineB})=20$ ,  $n_{\text{EXPRESSION}}(35\text{S:AtPAP27/lineD})=22$ ,  $n_{\text{EXPRESSION}}(35\text{S:AtPAP27/lineF})=7$ .



**Figure S8. AvgAbsAng measurements capture the variation in the top and bottom 5 accessions for "Direction Index" (A) and "Root Angle".** In each panel, the accessions with the highest "Direction Index" or "Root Angle" are shown on the left, while the accessions with the lowest "Direction Index" or "Root Angle" are shown on the right. n(Wa-1)=23, n(Cvi-0)=24, n(Kl-5)=24, n(Jm-0)=24, n(Eds-1)=18, n(Cala-8)=22, n(Yo-0)=21, n(Hh-0)=22, n(Rak-2)=20, n(Col-0)=22, n(Coc-1)=23.





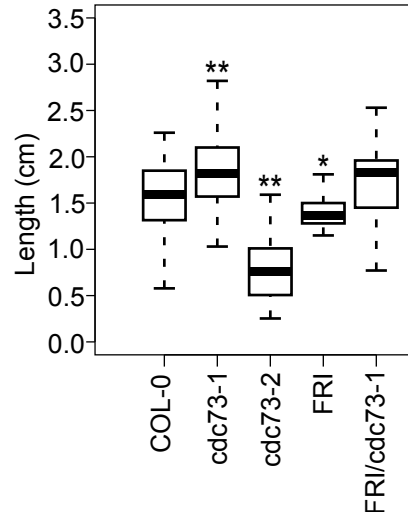


**Figure S10: Root length of *cdc73* mutant alleles does not vary in a manner similar to root angle.** Error bars represent standard error of the mean, n(Col-0)=144, n(cdc73-1)=85, n(cdc73-2)=26, n(FRI)=22, n(FRI/cdc73-1)=32. \* $p \leq 0.05$  \*\* $p \leq 0.01$  \*\*\* $p \leq 0.001$  as determined using an ANOVA.